FEBS Letters

FEBS PRESS science publishing by scientists

Wide-open conformation of UDP-MurNc-tripeptide ligase revealed by the substrate-free structure of MurE from *Acinetobacter baumannii*

Kyoung Ho Jung[1,2], Yeon-Gil Kim[3], Chang Min Kim[1,2], Hyun Ji Ha[1,2], Chang Sup Lee[4], Jun Hyuck Lee[5,6] and Hyun Ho Park[1,2]

1 Department of Global Innovative Drugs, Graduate School of Chung-Ang University, Seoul, Korea
2 College of Pharmacy, Chung-Ang University, Seoul, Korea
3 Pohang Accelerator Laboratory, Pohang University of Science and Technology, Korea
4 College of Pharmacy and Research Institute of Pharmaceutical Science, Gyeongsang National University, Jinju, Korea
5 Unit of Research for Practical Application, Korea Polar Research Institute, Incheon, Korea
6 Department of Polar Sciences, University of Science and Technology, Incheon, Korea

Correspondence
H. H. Park, College of Pharmacy, Chung-Ang University, Dongjak-gu, Seoul 06974, Korea
Tel: +82 2 820 5930
E-mail: xrayleox@cau.ac.kr
and
J. H. Lee, Unit of Research for Practical Application, Korea Polar Research Institute, Incheon 21990, Korea
Tel: +82 32 760 5555
E-mail: junhyucklee@kopri.re.kr

Kyoung Ho Jung and Yeon-Gil Kim contributed equally to this work.

(Received 24 September 2020, revised 22 October 2020, accepted 20 November 2020, available online 3 December 2020)

doi:10.1002/1873-3468.14007

Edited by Christian Griesinger

MurE ligase catalyzes the attachment of *meso*-diaminopimelic acid to the UDP-MurNAc-$_L$-Ala-$_D$-Glu using ATP and producing UDP-MurNAc-$_L$-Ala-$_D$-Glu-*meso*-A_2pm during bacterial cell wall biosynthesis. Owing to the critical role of this enzyme, MurE is considered an attractive target for antibacterial drugs. Despite extensive studies on MurE ligase, the structural dynamics of its conformational changes are still elusive. In this study, we present the substrate-free structure of MurE from *Acinetobacter baumannii*, which is an antibiotic-resistant superbacterium that has threatened global public health. The structure revealed that MurE has a wide-open conformation and undergoes wide-open, intermediately closed, and fully closed dynamic conformational transition. Unveiling structural dynamics of MurE will help to understand the working mechanism of this ligase and to design next-generation antibiotics targeting MurE.

Keywords: *Acinetobacter baumannii*; ATP-dependent ligase; cell wall peptidoglycan biosynthesis; crystal structure; MurE

Eubacteria contain a cell wall that is a structural layer surrounding the cell membrane [1]. This specific layer provides the bacterial cell with a structural boundary for protection and plays selective filter roles [1]. In bacteria, one of the major components of cell wall is peptidoglycans, which are formed by the polymerization of repeating disaccharide subunits cross-linked by short peptides [2,3]. Because the cell wall is critical for the viability of bacteria, peptidoglycan biosynthesis interference has become a successful strategy for effectively eliminating pathogenic bacteria [4,5]. For example, penicillins (beta-lactams), vancomycin (glycopeptides), and cycloserine, which are clinically used antibiotics, target this peptidoglycan biosynthesis pathway [4].

The process of peptidoglycan biosynthesis can be divided into three stages depending on the location

Abbreviations
MALS, multi-angle light scattering; MR, molecular replacement; SEC, size exclusion chromatography.

where the processes occur (cytoplasmic, membrane, and periplasmic stages) [1,3]. During the synthesis of peptidoglycan precursors in the cytoplasmic stage, four ATP-dependent ligases belonging to the Mur ligase family (MurC, MurD, MurE, and MurF) catalyze the addition of the peptide moiety to UDP-acetylmuramic acid (MurNAc), which is initially generated from UDP-acetylglucosamine (GlcNAc) by the MurA and MurB enzymes [6–8]. Assembly of the peptide moiety on UDP-MurNAc to generate UDP-MurNAc pentapeptides occurs by the successive addition of L-alanine by MurC, D-glutamine by MurD, diaminopimelic acid or L-lysine by MurE, and dipeptide D-alanyl-D-alanine by MurF [3,6,7,9]. Besides the individual function of Mur system, possibility of formation of multienzyme complex in Mur ligase family has been also suggested [7,9].

MurE catalyzes the attachment of *meso*-diaminopimelic acid (*meso*-A_2pm) to UDP-MurNAc-$_L$-Ala-$_D$-Glu (UAG) using ATP, producing UDP-MurNAc-$_L$-Ala-$_D$-Glu-*meso*-A_2pm (UMT), ADP, and P_i (Fig. 1A) [10,11]. This family of enzyme uses Mg^{2+} as cofactor. Kinetics study of MurE from *Escherichia coli* showed that Km values for *meso*-A_2pm and ATP were ~ 36 and 620 μM, respectively [12,13]. *Acinetobacter baumannii*, a causative agent of hospital-derived infections, is a 'superbug' that may lead to severe infections as its strains are resistant to multiple drugs [14,15]. In the present state of global health emergency, there is an urgent need for novel therapeutic agents against this pathogen.

In this study, to understand the molecular mechanism and obtain structural information for the design of next-generation antibiotics against *A. baumannii*, we characterized and elucidated the structure of the substrate- and nucleotide-free forms of MurE ligase from *A. baumannii* (abMurE). Based on the structural analysis and comparison with several MurE complex structures from different species [11,16–18], we revealed the novel wide-open

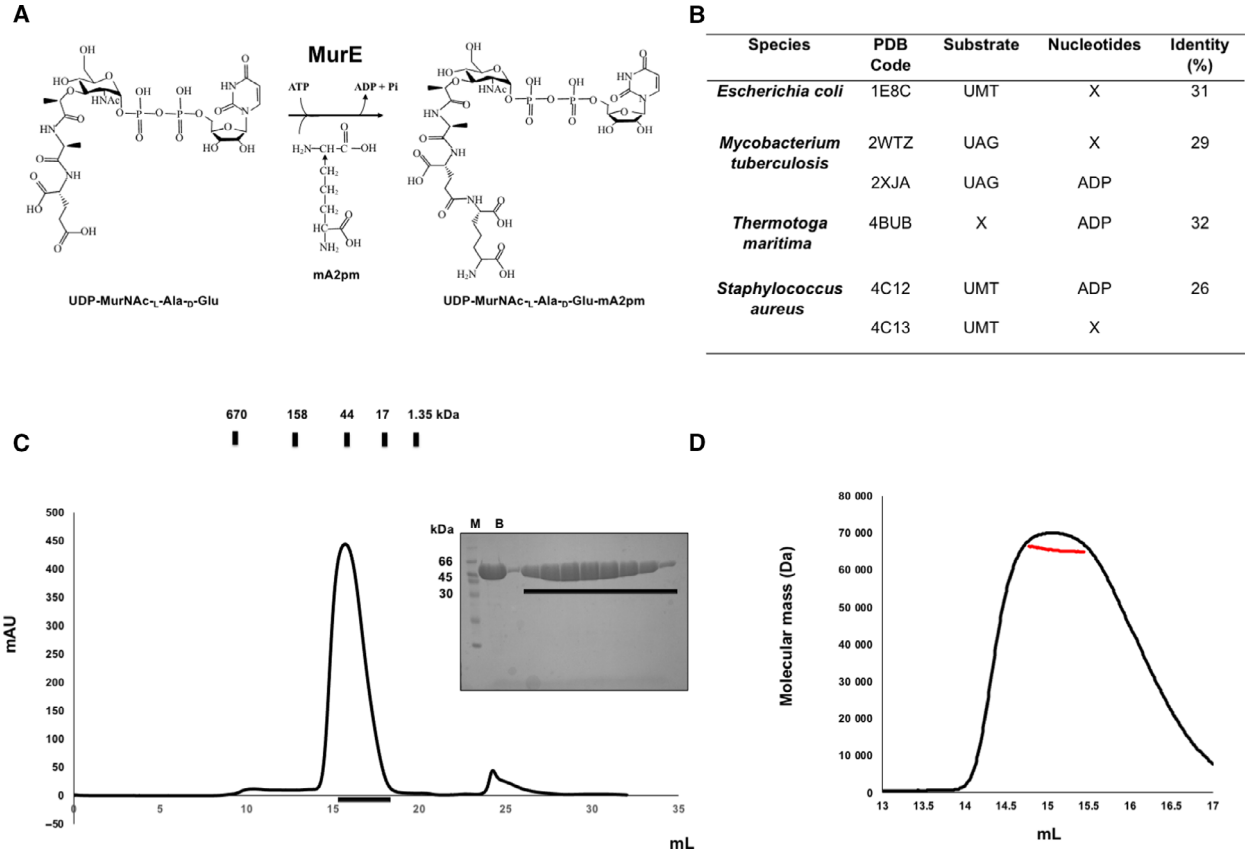

Species	PDB Code	Substrate	Nucleotides	Identity (%)
Escherichia coli	1E8C	UMT	X	31
Mycobacterium tuberculosis	2WTZ	UAG	X	29
	2XJA	UAG	ADP	
Thermotoga maritima	4BUB	X	ADP	32
Staphylococcus aureus	4C12	UMT	ADP	26
	4C13	UMT	X	

Fig. 1. Purification and characterization of MurE from *Acinetobacter Baumannii* (*abMurE*). (A) Overview of MurE function. (B) Table summarizing the current structural studies of the members of the MurE family. (C) Profile of SEC generated during purification of abMurE; SDS/PAGE for the verification and assessment of abMurE purity is shown to the right of the main peak. Loaded fractions are indicated by a black bar. M and B indicate the size marker and sample before SEC, respectively. (D) MALS profile derived from the main peak of the SEC. Red line indicates the experimental molecular weight analyzed by MALS.

conformation of MurE ligase. This wide-open structure of MurE indicates a dynamic structural transition between the open, intermediately closed, and fully closed transition states of the MurE family of ligases.

Materials and methods

Protein expression and purification

The full-length gene for MurE from *A. baumannii* (*abMurE*) (GeneBank ID: ADX05085.1) was synthesized by BIONICS (Seoul, Republic of Korea) and cloned into a pET21a expression vector. The plasmid encoding the full-length *abMurE* was transformed into *E. coli* BL21 (DE3) cells. A single colony was selected and cultured overnight at 37 °C in 5 mL lysogeny broth (LB) containing 50 $\mu g \cdot mL^{-1}$ kanamycin, following which the cells were transferred and cultured in 1 L medium. When the optical density (OD) value at 600 nm reached approximately 0.6, 0.5 mM isopropyl β-D-1-thiogalactopyranoside (IPTG) was added into the medium for target gene induction. The induced cells were further cultured for 18 h at 20 °C and harvested by centrifugation at 20 °C. The collected cells were resuspended with 40 mL lysis buffer [20 mM Tris/HCl (pH 8.0) and 500 mM NaCl]. After adding 1 mM PMSF (Sigma-Aldrich, St. Louis, MO, USA), the cells were disrupted by sonication on ice with six bursts of 30 s each and a 60 s interval between two bursts. The lysed cell suspension was centrifuged at 10 000 ***g*** for 30 min at 4 °C to remove cell debris. The collected supernatant was then mixed with nickel nitrilotriacetic acid (Ni-NTA) resin (Qiagen, Hilden, Germany) by gentle agitation for 1 h at 4 °C. The resulting mixture was applied to a gravity-flow column pre-equilibrated with lysis buffer. The column was washed with 100 mL of washing buffer [20 mM Tris/HCl (pH 8.0), 500 mM NaCl, and 25 mM imidazole]. Next, a total of 3 mL of elution buffer [20 mM Tris/HCl (pH 7.9), 500 mM NaCl, and 250 mM imidazole] was loaded onto the column to elute the bound protein. The resulting eluate was concentrated to 30 $mg \cdot mL^{-1}$ and sequentially subjected to size exclusion chromatography (SEC). SEC purification was conducted using an ÄKTA Explorer system (GE Healthcare, Chicago, IL, USA) equipped with a Superdex 200 Increase 10/300 GL 24 mL column (GE Healthcare) pre-equilibrated with SEC buffer [20 mM Tris/HCl (pH 8.0), 150 mM NaCl]. Protein fractions were collected, concentrated to 10.9 $mg \cdot mL^{-1}$, flash-frozen in liquid N_2, and stored at −80 °C until use.

SEC-MALS analysis

The absolute molar mass of abMurE in solution was determined by multi-angle light scattering (MALS). The target protein filtered with a 0.2-μm syringe filter was loaded onto a Superdex 200 10/300 gel-filtration column (GE Healthcare) that had been pre-equilibrated in a buffer comprising 20 mM Tris/HCl (pH 8.0) and 150 mM NaCl. The mobile phase buffer flowed at a rate of 0.4 $mL \cdot min^{-1}$ at 25 °C. A DAWN-treos MALS detector (Wyatt Technology, Santa Barbara, CA, USA) was connected with the ÄKTA explorer system (GE Healthcare). The molecular mass of bovine serum albumin was used as a reference value. Data for the absolute molecular mass were assessed using the ASTRA program (Wyatt Technology).

Crystallization and data collection

For initial crystallization, 1 μL of protein solution was mixed with an equal volume of reservoir solution, and the droplet was allowed to equilibrate against 400 μL of the mother liquor using the hanging drop vapor diffusion method at 20 °C. The crystal was obtained from a buffer comprising 21% (v/v) 2-propanol, 30% (v/v) glycerol, 0.07 M sodium cacodylate trihydrate pH 6.5, and 0.14 M sodium citrate tribasic dihydrate. Qualified crystals appeared in 22 days and grew to a maximum size of 0.3 × 0.1 × 0.1 mm^3. For data collection, the crystals were flash-cooled in a stream of N_2 at −178 °C. X-ray diffraction data were collected at the Pohang Accelerator Laboratory with the 5C beamline (Pohang, Republic of Korea) at a wavelength of 1.0000 Å. The diffraction data were indexed, integrated, and scaled with the HKL-2000 program [19].

Structure determination and analysis

PHASER [20] in PHENIX package [21] was used for the molecular replacement (MR) phasing method to determine the structure. Two separated domains, the N-terminal-central and C-terminal domains of the previously solved MurE/ADP complex structure (PDB ID: 4BUB) [22], which shares 32% sequence homology with abMurE, were used as an individual search model. The initial model was constructed automatically with AUTOBUILD in PHENIX [21] and completed with COOT [23]. Model refinement was iteratively performed using PHENIX.REFINE of the PHENIX package [21]. The quality of the model was validated using MOLPROBITY [24]. Structural representations were generated using the PYMOL program [25]. The angle of domain movement was analyzed using DYNDOM3D [26].

Structural data accession number

Coordinate and structural factors were deposited in the Protein Data Bank under PDB ID: 7D27.

Results and Discussion

Overall structure of abMurE

To further understand the mechanisms underlying the function of MurE, we elucidated the substrate- and nucleotide-free structures of MurE after its purification

using a quick two-step chromatography. The final protein sample used for crystallization was eluted approximately 16–17 mL position from the SEC column, indicating that abMurE exists as a monomer in solution. To confirm the stoichiometric state of abMurE in solution, we analyzed the absolute molecular weight using MALS. The experimental molecular weight of abMurE in solution was 62.3 kDa (2.01% fitting error) (Fig. 1D). As the theoretically calculated molecular weight of the monomeric full-length abMurE (residues 1–499), including the C-terminal His-tag, is 58.4 kDa, we concluded that the working stoichiometry of abMurE is a monomer in solution.

The purified and characterized abMurE was crystallized, and the crystal structure of full-length abMurE at 2.48 Å resolution was elucidated using the MR phasing method. At the initial stage of structural determination, the previously reported structure of MurE from *Thermotoga maritima* (PDB ID: 4BUB) [22], sharing 32% sequence identity with abMurE, was used for the MR search model. However, we did not obtain a reasonable solution from MR. Mur family ligases (including MurE) possess a similar domain organization, with an N-terminal domain responsible for binding UDP-MurNAc-peptide precursors, a central domain responsible for binding ATP, and a C-terminal domain responsible for binding the amino acids to be added onto the precursor [6,22], and C-terminal domain changes its location by binding to the substrate and nucleotide [3,6,9,22]. We therefore divided the full-length MurE search model into two parts, an N-terminal and central domain and a C-terminal domain. By using these two parts separately, we first found a correct solution with N-terminal and central domain search model, following which we found a solution with a C-terminal domain search model. The two separately found solutions were combined and a final model was generated. The final structure was refined to R_{work} = 21.43% and R_{free} = 25.70%. The crystallographic and refinement statistics are summarized in Table 1. A single molecule was present in the asymmetric unit, and the final structural model was constructed from residues 2 to 491 (Fig. 2A). Although the expressed gene contains the full-length abMurE, 16 residues containing poly-histidine tags at the C-terminus and several loops formed by residues 43–46, 148–153, and 205–208 were not included in the final model owing to untraceable electron density (Fig. 2A). The abMurE structure was composed of 15 α-helixes (H1–H15), 21 β-strands (S1–S21), and connecting loops (Fig. 2A) forming three distinct domains, an N-terminal domain (residues 1–98), a central domain (residues 103–331), and a C-terminal domain (residues 337–491) (Fig. 2B). B-factor analysis showed that the previously identified UAG substrate binding region located between the N-terminal and central domains was the highest B-factor region, indicating that several flexible loops of abMurE mediated the interaction with the UAG substrate (Fig. 2C). Sequence and structural surface analyses also indicated that a typical ATP binding site (GxxGKT motif) and two substrate binding sites, UAG and mA2pm, were conserved in the abMurE structure by forming proper binding pockets on the surface of the enzyme (Fig. 2D,E).

Table 1. Data collection and refinement statistics.

Data collection	
Space group	$P4_22_12$
Unit cell parameter *a*, *b*, *c* (Å)	
a, *b*, *c* (Å)	*a* = 119.96, *b* = 119.96, *c* = 116.73
α, β, γ (°)	α = 90, β = 90, γ = 90
Resolution range (Å)[a]	29.18–2.48
Total reflections	544 491
Unique reflections	30 793
Multiplicity	17.7 (17.4)
Completeness (%)[a]	100.0 (100.0)
Mean $I/\sigma(I)$[a]	20.4 (1.9)
R_{merge}[a,b]	0.096 (1.728)
R_{meas}	0.099 (1.780)
R_{pim}	0.023 (0.424)
$CC_{1/2}$	0.934 (0.695)
Wilson B-factor (Å[b])	24.91
Refinement	
Resolution range (Å)	19.99–2.48
Reflections	30 726
R_{work} (%)	21.43 (27.73)
R_{free} (%)	25.70 (32.13)
No. of molecules in the asymmetric unit	1
No. of nonhydrogen atoms	3716
Protein	3696
Solvent	20
Average B-factor values (Å[b])	30.18
Protein	30.12
Solvent	25.48
Ramachandran plot	
Favored/allowed/outliers (%)	96.79/3.21/0
Rotamer outliers (%)	0.51
Clashscore	6.69
RMS deviation from ideal values	
Bonds lengths (Å)	0.009
Bonds angles (°)	0.958
Dihedral angle (°)	3.207

[a]Values for the outermost resolution shell in parentheses.; [b]$R_{merge} = \Sigma_h \Sigma_i |I(h)_i - \langle I(h)\rangle| / \Sigma_h \Sigma_i I(h)_i$, where $I(h)$ is the observed intensity of reflection h and $\langle I(h)\rangle$ the average intensity obtained from multiple measurements.

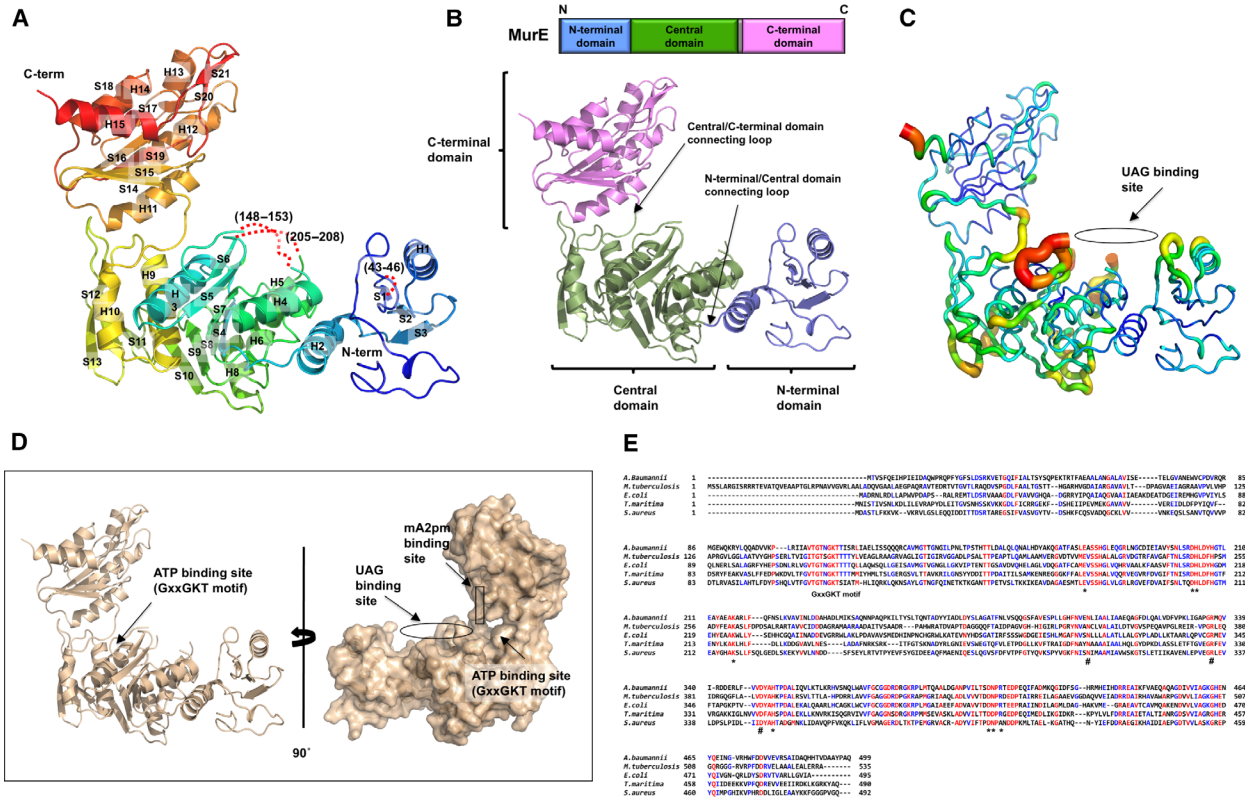

Fig. 2. Overall structure of abMurE. (A) Rainbow-colored cartoon representation of monomeric abMurE. The chain from the N- to C-terminal is colored blue to red. Helices and sheets are labeled with H and S, respectively. (B) Cartoon representation of the abMurE structure showing the domain boundaries. (C) Putty representation showing B-factor distribution on the abMurE structure. B-factor value order is shown in rainbow color from red (high value) to blue (low value). Black oval indicates the substrate binding site. (D) Surface feature of abMurE. The UAG, mA2pm, and ATP binding sites are indicated by black arrows. (E) Sequence alignment of MurE from various bacterial species. Completely and partially conserved residues are indicated by red and blue color, respectively. GxxGKT motif, important for nucleotide binding, is indicated. Other residues that are involved in the nucleotide binding are indicated by sharp mark. Star mark indicates residues involved in the substrate interaction.

Structural comparison of abMurE with MurE from different species

To investigate the molecular mechanism of activity control and the structural dynamics of MurE, we compared it to its structural homologs searched by the Dali server (Table 2) [27]. Although the structures of MurE from four different species, *T. maritima* (tmMurE), *Mycobacterium tuberculosis* (mtMurE), *Staphylococcus aureus* (saMurE), and *E. coli* (ecMurE) are selected as the best matches from Dali server [11,16,18,22], the previously reported MurE structures from different species were complexes containing either the substrate (or product) or nucleotide (Fig. 1B and Table 2). Those structures include the following: ecMurE/UMT (PDB ID: 1E8C) [11], mtMurE/UAG (PDB ID: 2WTZ) [18], mtMurE/UAG-ADP (PDB ID: 2XJA) [17], tmMurE/ADP (PDB ID: 4BUB) [22], saMurE/UMT (PDB ID: 4C12) [16], and saMurE/UMT-ADP complexes (PDB ID: 4C13) [16]. Our current abMurE structure is the first to show the substrate- and nucleotide-free form of MurE. Based on

Table 2. Structural similarity search using the Dali server [27].

Proteins (accession number)	*Z*-score	RMSD (Å)	Identity (%)	References
MurE from *T. maritima* (4BUB)	34.9	5.7	33	[22]
MurE from *M. tuberculosis* (2WTZ)	34.2	5.6	29	[18]
MurE from *S. aureus* (4C12)	33.8	6.5	26	[16]
MurE from *E. coli* (1E8C)	31.8	6.4	31	[11]
MurE from *M. tuberculosis* (2XJA)	31.5	3.4	29	[17]

Dali server searches, nucleotide (ADP)-bound tmMurE was the most structurally similar protein (Table 2).

Structural comparison of abMurE with the tmMurE/ADP complex by superpositioning showed that the two structures were not identical, exhibiting a RMSD of 5.7 Å over 490 Cα atoms, although the sequence identity between abMurE and tmMurE was 32%, and the domain composition with three distinct domains was the same (Fig. 3A). This structural deviation derived from a structurally mismatched C-terminal domain translocated by approximately 35° toward the exterior from the central domain. This indicates that the substrate- and nucleotide-free form of abMurE has a wide-open structure of the MurE family, which has not been detected in other MurE family members from different species (Fig. 3A). Pairwise superimposition analysis of abMurE with various MurE ligases from different species also showed that the C-terminal domain of the substrate- and nucleotide-free form of abMurE was dislocated from the C-terminal domain of the substrate/nucleotide complex form of other MurG structures by approximately 35°–50°, confirming that the structure of abMurE, the first substrate- and nucleotide-free form of MurE to be described, is wide-open (Fig. 3B–E).

Wide-open conformation of MurE without the nucleotide or substrate that undergoes wide-open, intermediately closed, and fully closed dynamic conformational transition

Dynamic conformational changes upon substrate binding is a common feature of the Mur family of bacterial cell wall ligases [6]. Structural studies of the Mur family, including MurC, MurD, and MurF, indicate that the Mur ligase has an open conformation when not bound to the substrate or nucleotide. Once the substrate or nucleotide binds to the enzyme, it shows a closed conformation by moving the C-terminal domain that surrounds the substrate. In the Mur family of ligases, MurE is known to be the most structurally unchanged ligase upon substrate or product binding [22]. Although the movement of the C-terminal domain of the MurE enzyme is minimal, the substrate (UAG)- or product (UMT)-bound MurE is considered to have a closed conformation, while the nucleotide (ADP)-bound MurE has been suggested to possess an open conformation [9,16,28,29]. In the nucleotide- and substrate-free structure of MurE determined in the current study, the open conformation was formed without binding to any molecule. The nucleotide-binding structure of MurE, considered an open conformation, may be an intermediate form of the MurE enzyme. Our structural superposition analysis showed that in MurE structures from various species, the C-terminal domain was moved toward the central and N-terminal domains by approximately 35° upon ADP binding, ~ 40°–45° upon UAG or UAG/ADP binding, and ~ 50°–55° upon UMT or UMT/ADP binding (Fig. 4A). The existence of a nucleotide-bound intermediate form of the Mur ligase has been previously suggested for the MurF family. The structural study of MurF from *T. maritima* complexed with ADP revealed that the C-terminal domain is located between the closed and open structures, indicating that MurF forms an intermediate conformation after binding the nucleotide [22]. Phylogenetic analysis of homologous MurE sequences from various species using the ConSurf server [30] indicated that the residues involved in the formation of the central/C-terminal domain connecting loop, which is critical for the movement of the C-terminal domain, were conserved, making the loop a functionally important region (Fig. 4B). Recent study indicated that each family of Mur ligase can form a complex each other. In the case of *Streptococcus pneumoniae,* MurE interacted with MurC, MurD, and MurF [7]. This structural plasticity of the MurE ligase under nucleotide or substrate binding could modulate the affinity between the different components of the Mur system.

In conclusion, because of its involvement in the peptidoglycan biosynthesis pathway and essential role in maintaining cell viability, the Mur ligase family, including MurE, is considered an attractive target for antibacterial therapeutic interventions [5,9,17]. MurE has a wide-open conformation without the nucleotide or substrate. When the nucleotide binds to MurE, the C-terminal domain of MurE moves slightly toward the central domain, forming an intermediately closed conformation. Finally, MurE reaches a fully closed conformation by accommodating the substrate. This open, intermediately closed, and fully closed dynamic conformational transition is critical for the function of MurE, and it is conserved in most bacterial MurE.

Fig. 3. Structural comparison of substrate- and nucleotide-free abMurE with MurE enzymes from different species complexed with substrate, product, and nucleotide. (A–E) Pairwise structural superimposition of abMurE with tmMurE/ADP (A), mtMurE/UAG (B), mtMurE/UAG/ADP (C), ecMurE/UMT (D), and saMurE/UMT/ADP complexes (E).

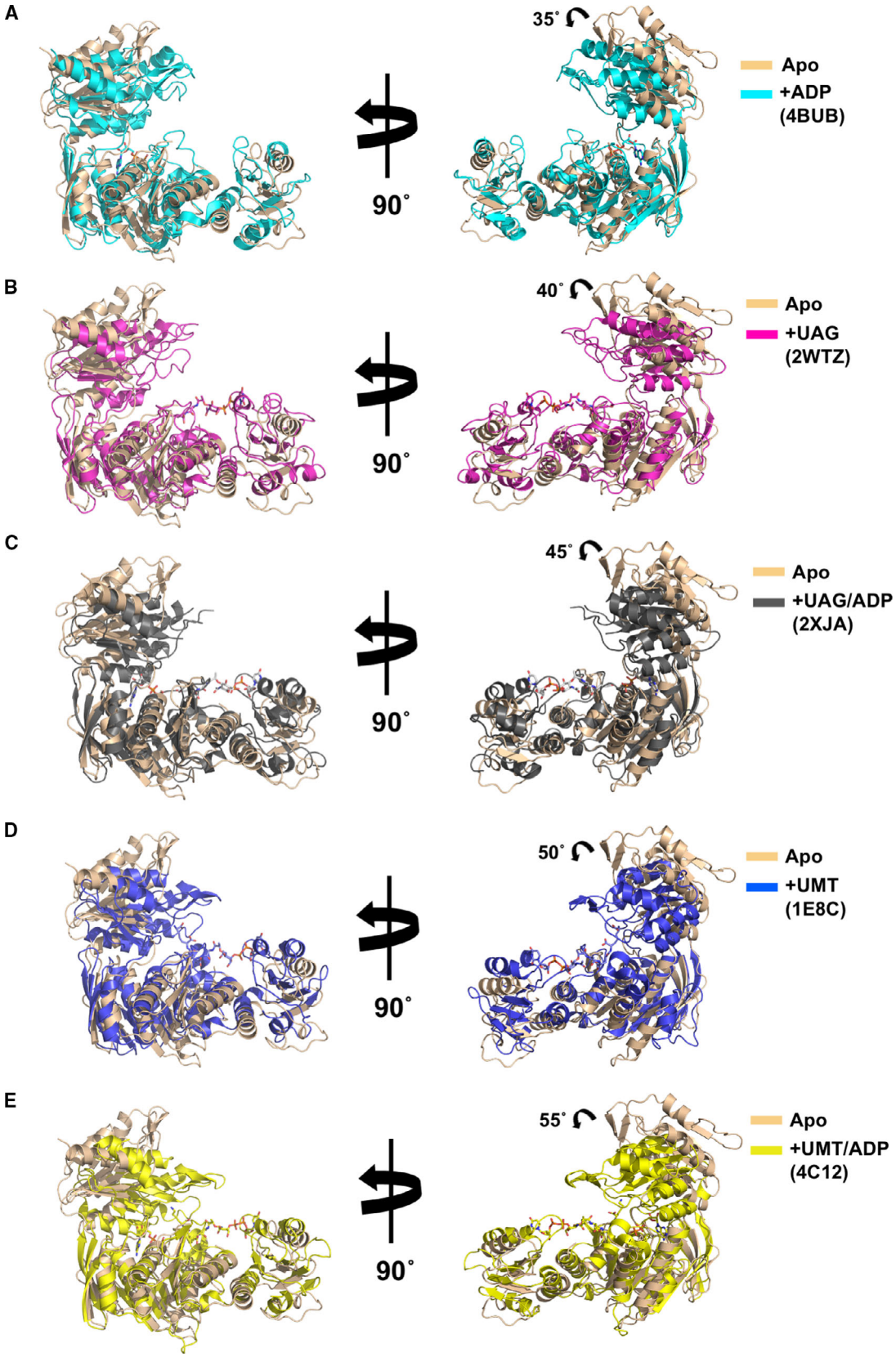
A
35˚
Apo
+ADP
(4BUB)
90˚
B
40˚
Apo
+UAG
(2WTZ)
90˚
C
45˚
Apo
+UAG/ADP
(2XJA)
90˚
D
50˚
Apo
+UMT
(1E8C)
90˚
E
55˚
Apo
+UMT/ADP
(4C12)
90˚

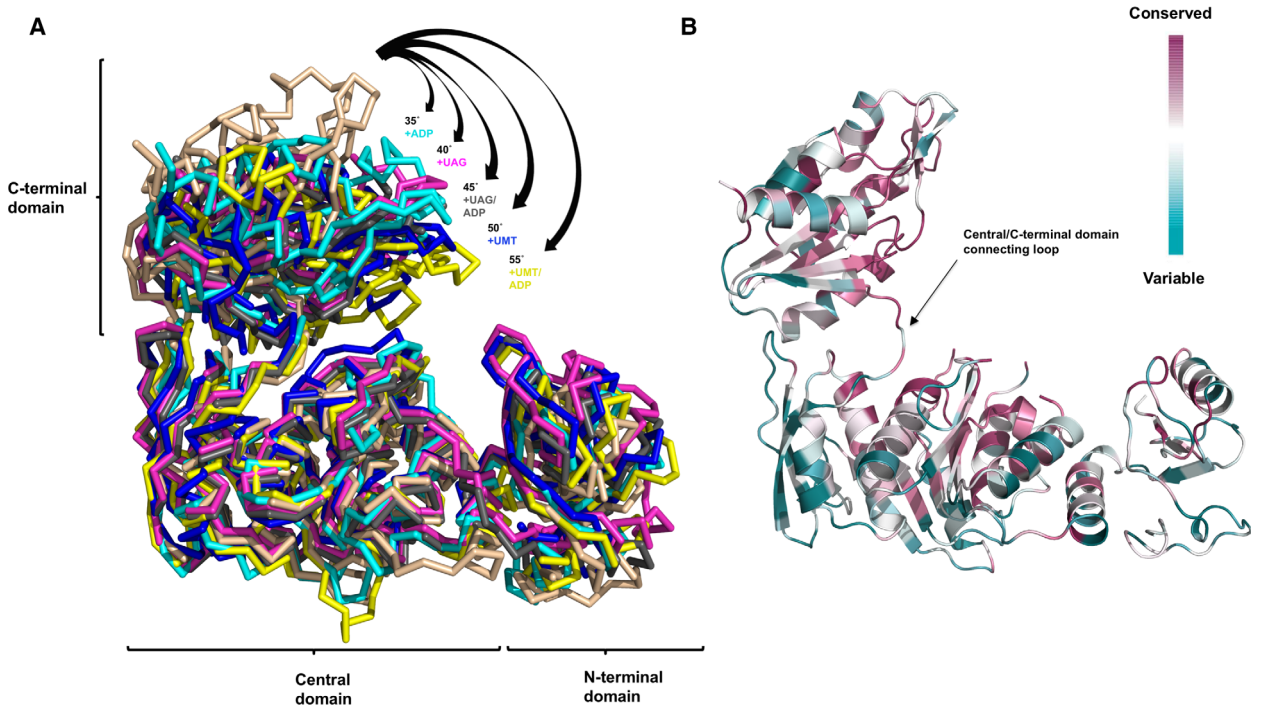

Fig. 4. Conformational changes of the C-terminal domain of MurE upon binding with substrate and nucleotide. (A) Structural superimposition of the wide-open conformation of the substrate- and nucleotide-free form of abMurE with different forms of MurE. The color code shown is the same as in Fig. 3. The rotation angles of the C-terminal domain of MurE upon binding to ADP, UAG, and UMT are indicated with black curved arrows. (B) Cartoon representation of abMurG with colors indicating the degree of amino acid sequence conservation.

The transition occurs through a conserved central/C-terminal domain connecting loop that controls the movement of the C-terminal domain.

Acknowledgements

This work was supported by the Basic Science Research Program of the National Research Foundation of Korea (NRF) of the Ministry of Education, Science, and Technology [grant numbers NRF-2017M3A9D8062960, NRF-2018R1A4A1023822, and NRF-2018R1A2B2003635] and the Korea Polar Research Institute [grant number PM20030].

Author contributions

HHP and JHL designed and supervised the project. KHJ performed cloning, expression, and protein purification. HHJ, HJH, and Y-GK crystallized and collected X-ray data. KHJ, Y-GK, and HHP solved the protein structure. CSL performed MALS and constructed the chemical reaction figure. HHP and JHL wrote the manuscript. All the authors discussed the results and commented on and approved the manuscript.

References

1 Typas A, Banzhaf M, Gross CA and Vollmer W (2011) From the regulation of peptidoglycan synthesis to bacterial growth and morphology. *Nat Rev Microbiol* **10**, 123–136.
2 Vollmer W and Bertsche U (2008) Murein (peptidoglycan) structure, architecture and biosynthesis in *Escherichia coli*. *Biochim Biophys Acta* **1778**, 1714–1734.
3 Mattei PJ, Neves D and Dessen A (2010) Bridging cell wall biosynthesis and bacterial morphogenesis. *Curr Opin Struct Biol* **20**, 749–755.
4 Matsumoto H, Takechi K, Sato H, Takio S and Takano H (2012) Treatment with antibiotics that interfere with peptidoglycan biosynthesis inhibits chloroplast division in the desmid *Closterium*. *PLoS One* **7**, e40734.
5 Chung BC, Mashalidis EH, Tanino T, Kim M, Matsuda A, Hong J, Ichikawa S and Lee SY (2016) Structural insights into inhibition of lipid I production in bacterial cell wall synthesis. *Nature* **533**, 557–560.

6 Smith CA (2006) Structure, function and dynamics in the mur family of bacterial cell wall ligases. *J Mol Biol* **362**, 640–655.
7 Miyachiro MM, Granato D, Trindade DM, Ebel C, Leme AFP and Dessen A (2019) Complex formation between Mur enzymes from *Streptococcus pneumoniae*. *Biochemistry* **58**, 3314–3324.
8 Bupp K and Vanheijenoort J (1993) The final step of peptidoglycan subunit assembly in *Escherichia coli* occurs in the cytoplasm. *J Bacteriol* **175**, 1841–1843.
9 Kouidmi I, Levesque RC and Paradis-Bleau C (2014) The biology of Mur ligases as an antibacterial target. *Mol Microbiol* **94**, 242–253.
10 Abo-Ghalia M, Michaud C, Blanot D and van Heijenoort J (1985) Specificity of the uridine-diphosphate-N-acetylmuramyl-L-alanyl-D-glutamate: meso-2,6-diaminopimelate synthetase from *Escherichia coli*. *Eur J Biochem* **153**, 81–87.
11 Gordon E, Flouret B, Chantalat L, van Heijenoort J, Mengin-Lecreulx D and Dideberg O (2001) Crystal structure of UDP-N-acetylmuramoyl-L-alanyl-D-glutamate: meso-diaminopimelate ligase from *Escherichia coli*. *J Biol Chem* **276**, 10999–11006.
12 Michaud C, Menginlecreulx D, Vanheijenoort J and Blanot D (1990) Over-production, purification and properties of the uridine-diphosphate-N-acetylmuramoyl-L-alanyl-D-glutamate – meso-2,6-diaminopimelate ligase from *Escherichia coli*. *Eur J Biochem* **194**, 853–861.
13 Menginlecreulx D, Blanot D and Vanheijenoort J (1994) Replacement of diaminopimelic acid by cystathionine or lanthionine in the peptidoglycan of *Escherichia coli*. *J Bacteriol* **176**, 4321–4327.
14 Burki TK (2018) Superbugs: an arms race against bacteria. *Lancet Respir Med* **6**, 668.
15 Kumar M (2016) Resistant superbugs: race against time. *Infect Control Hosp Epidemiol* **37**, 365–366.
16 Ruane KM, Lloyd AJ, Fulop V, Dowson CG, Barreteau H, Boniface A, Dementin S, Blanot D, Mengin-Lecreulx D, Gobec S *et al.* (2013) Specificity determinants for lysine incorporation in *Staphylococcus aureus* peptidoglycan as revealed by the structure of a MurE enzyme ternary complex. *J Biol Chem* **288**, 33439–33448.
17 Basavannacharya C, Moody PR, Munshi T, Cronin N, Keep NH and Bhakta S (2010) Essential residues for the enzyme activity of ATP-dependent MurE ligase from *Mycobacterium tuberculosis*. *Protein Cell* **1**, 1011–1022.
18 Basavannacharya C, Robertson G, Munshi T, Keep NH and Bhakta S (2010) ATP-dependent MurE ligase in *Mycobacterium tuberculosis*: biochemical and structural characterisation. *Tuberculosis* **90**, 16–24.
19 Otwinowski Z and Minor W (1997) Processing of X-ray diffraction data collected in oscillation mode. *Methods Enzymol* **276**, 307–326.
20 McCoy AJ (2007) Solving structures of protein complexes by molecular replacement with Phaser. *Acta Crystallogr D* **63**, 32–41.
21 Adams PD, Afonine PV, Bunkoczi G, Chen VB, Davis IW, Echols N, Headd JJ, Hung LW, Kapral GJ, Grosse-Kunstleve RW *et al.* (2010) PHENIX: a comprehensive Python-based system for macromolecular structure solution. *Acta Crystallogr D* **66**, 213–221.
22 Favini-Stabile S, Contreras-Martel C, Thielens N and Dessen A (2013) MreB and MurG as scaffolds for the cytoplasmic steps of peptidoglycan biosynthesis. *Environ Microbiol* **15**, 3218–3228.
23 Emsley P and Cowtan K (2004) Coot: model-building tools for molecular graphics. *Acta Crystallogr D* **60**, 2126–2132.
24 Chen VB, Arendall WB III, Headd JJ, Keedy DA, Immormino RM, Kapral GJ, Murray LW, Richardson JS and Richardson DC (2010) MolProbity: all-atom structure validation for macromolecular crystallography. *Acta Crystallogr D* **66**, 12–21.
25 DeLano WL and Lam JW (2005) PyMOL: a communications tool for computational models. *Abstr Pap Am Chem S* **230**, U1371–U1372.
26 Girdlestone C and Hayward S (2016) The DynDom3D webserver for the analysis of domain movements in multimeric proteins. *J Comput Biol* **23**, 21–26.
27 Holm L and Sander C (1995) Dali: a network tool for protein structure comparison. *Trends Biochem Sci* **20**, 478–480.
28 Bansal R, Haque MA, Hassan MI, Ethayathulla AS and Kaur P (2020) Structural and conformational behavior of MurE ligase from *Salmonella enterica* serovar Typhi at different temperature and pH conditions. *Int J Biol Macromol* **150**, 389–399.
29 Bansal R, Haque MA, Yadav P, Gupta D, Ethayathulla AS, Hassan MI and Kaur P (2018) Estimation of structure and stability of MurE ligase from *Salmonella enterica* serovar Typhi. *Int J Biol Macromol* **109**, 375–382.
30 Ashkenazy H, Abadi S, Martz E, Chay O, Mayrose I, Pupko T and Ben-Tal N (2016) ConSurf 2016: an improved methodology to estimate and visualize evolutionary conservation in macromolecules. *Nucleic Acids Res* **44**, W344–W350.